

New developments in FLUKA modelling of hadronic and EM interactions

A. Fassò*, A.Ferrari#, J. Ranft†, P.R.Sala#

* SLAC, Radiation Physics Department, ms 48, P.O. Box 4349, Stanford CA94309, USA

INFN sez. di Milano, via Celoria 16, I-20133 Milano, Italy

† Laboratori Nazionali del Gran Sasso, Assergi (AQ), Italy

Abstract

Recent developments in the FLUKA code are outlined. Charged particle energy losses below an (arbitrary) explicit δ ray production threshold are obtained from a sophisticated statistical approach which includes “close” collisions, plus a two-oscillators model for “distant” collisions; comparison with experimental energy loss straggling are presented. Several improvements took place in the PEANUT hadronic generator, among which the inclusion of new processes mainly triggered by the needs of the ICARUS experiment. Standard and exotic nucleon decay channels are now available with full simulation of the intranuclear effects and their influence on the final state configuration. Negative muon capture at rest is also described, and the implementation of neutrino nuclear interactions, with particular care in the treatment of nuclear Fermi motion and hadron formation time effects is in progress. The calculation of residual nuclei has been refined and extended also to neutron interactions below 20 MeV, including fission, with suitable modifications to the multigroup library.

A few only of these topics are presented in the text, because of space reasons. Other details about some of the FLUKA applications can be found in a companion paper at this conference [1].

1 Ionization energy losses

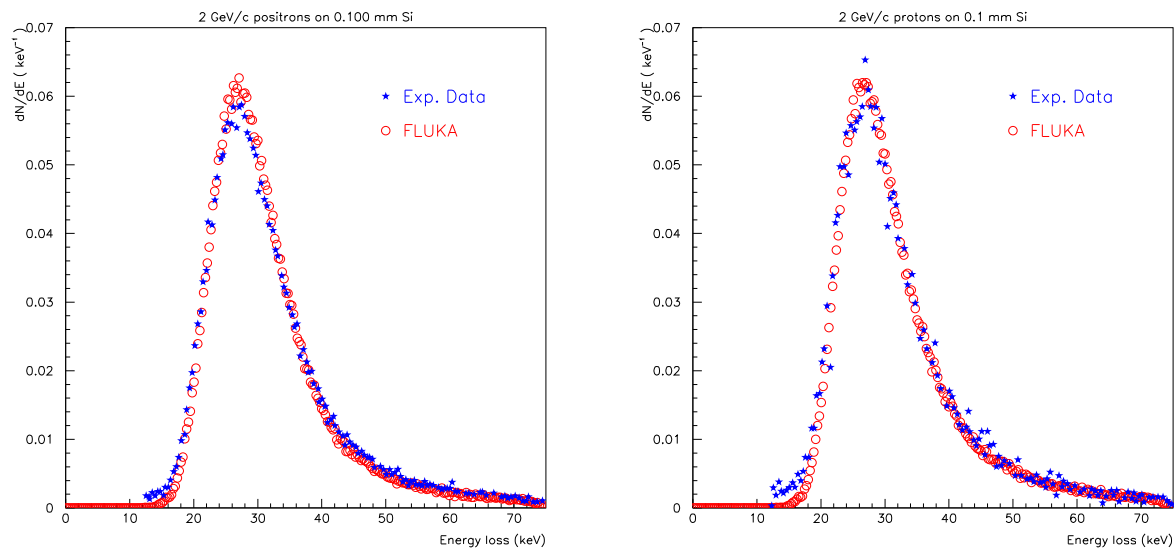


Figure 1: Experimental [14] and calculated energy loss distributions for 2 GeV/c positrons (left) and protons(right) traversing $100\mu\text{m}$ of Si.

The fluctuations associated with charged particle energy losses are a classical topic. However the most popular solutions are of difficult application in MonteCarlo approaches. The Landau [2] distribution has several limitations which restrict its use to a limited number of situations:

- The maximum energy of produced δ rays is assumed to be infinite \rightarrow a proper cut on the maximum loss has to be applied to ensure the correct average energy loss and the Landau distribution cannot be applied for too long steps and/or low velocities where the maximum secondary electron energy cannot be assumed to be very large
- The underlying δ cross section for “close” collisions is assumed to be simply $\propto \frac{1}{T_e^2}$ where T_e is the secondary electron kinetic energy \rightarrow differences among the cross sections for different particles are neglected
- The fluctuations connected with “distant” collisions are neglected, \rightarrow the Landau distribution cannot be applied for too short steps where “distant” collision fluctuations dominate

The use of the Vavilov [3] approach overcomes only the first problem at the price of a significant increase in computational complexity which prevent any practical use whenever the step length and/or the particle energies are not known a priori. Simple corrections for the third point [5] increase only marginally the range of applicability [4, 9] and force to use phenomenological correction factors [6] to bring back the simulated data in agreement with the experimental ones.

An alternative approach has been devised for FLUKA which makes use of very general statistical properties of the problem. Within this framework “practical” solutions have been implemented into the code with very satisfactory results. This approach exploits the properties of the cumulants [7] of distributions, and in particular of the cumulants of the distribution of Poisson distributed variables. Given a Poisson distributed number of events n , each one described by a distribution $P(x)$, with given $\langle n \rangle$, $\langle x^m \rangle$, $m = 1, \dots$ the following fundamental relations hold for the statistical variable $y = \sum_{i=1}^n x_i$:

$$\begin{aligned}\langle y \rangle &= \langle n \rangle \langle x \rangle \\ \sigma_y^2 &\equiv \langle y^2 \rangle - \langle y \rangle^2 = \langle n \rangle \langle x^2 \rangle\end{aligned}$$

which can be shown [8] to be generalized to all the cumulants k_m of the distribution:

$$k_m(y) = \langle n \rangle \langle x^m \rangle \quad (1)$$

Let η be a suitable lower threshold for close collisions, below which the distant collision description must be used, and let us assume as usual that distant collisions are described by N_d discrete levels E_i for excitation and ionization, with oscillator strengths f_i and microscopic cross sections σ_i . Using the general relation 1 and with the only limitation that the energy loss suffered by a particle along the step t is small compared to the initial energy, it can be shown [8] that the m th cumulant of the energy loss distribution, $k_m^{\Delta E}$ can be expressed by:

$$k_m^{\Delta E} = \sum_{i=1}^{N_d} \langle n_i \rangle E_i^m + \langle n_\delta^{T_{min}} \rangle \langle T_\delta^m \rangle \quad (2)$$

$$\langle n_i \rangle = n_e \sigma_i t \equiv \Sigma_i t \quad (3)$$

$$\langle n_\delta^{T_{min}} \rangle = n_e t \int_\eta^{T_{min}} dT_e \frac{d\sigma_\delta}{dT_e} \quad (4)$$

$$\langle T_\delta^m \rangle = n_e t \int_\eta^{T_{min}} dT_e T_e^m \frac{d\sigma_\delta}{dT_e} \quad (5)$$

$$n_e = \sum_{j=1}^L \frac{Z_j \rho_j N_A}{A_j} \quad (6)$$

where T_{min} is the threshold for explicit δ ray production, $d\sigma_\delta/dT_e$ the cross section for δ ray production, n_e the number of electrons per unit volume, N_A the Avogadro number, L the number of elements of the mixture or compound under consideration, and Z_j , A_j , and ρ_j their atomic numbers, atomic weight, and partial densities respectively.

Recalling the relations among the cumulants, k_m , and the central moments, μ_m , of a distribution [7]:

$$\begin{aligned}k_1 &= \langle x \rangle ; \mu_1 = 0 \\ k_2 &= \mu_2 ; \mu_2 = k_2 \\ k_3 &= \mu_3 ; \mu_3 = k_3 \\ k_4 &= \mu_4 - 3\mu_2^2 ; \mu_4 = k_4 + 3k_2^2\end{aligned} \quad (7)$$

$$\begin{aligned}
k_5 &= \mu_5 - 10\mu_3\mu_2 ; \mu_5 = k_5 + 10k_3k_2 \\
k_6 &= \mu_6 - 15\mu_4\mu_2 - 10\mu_3^2 + 30\mu_2^3 ; \mu_6 = k_6 + 15k_4k_2 + 10k_3^2 + 15k_2^3 \\
&\dots
\end{aligned}$$

it is easy to derive from eq. 2 whichever moment of the energy loss distribution.

In particular, assuming [9, 10] for σ_i :

$$\sigma_i = \frac{2\pi r_e^2 m_e c^2}{\beta^2 E_i} f_i \left[\log \frac{2m_e c^2 \beta^2 \gamma^2}{E_i} - 0.577 - \delta_i \right] \quad (8)$$

$$\sum_{i=1}^{N_d} f_i \log E_i \equiv \log I \quad (9)$$

$$\sum_{i=1}^{N_d} f_i = 1 \quad (10)$$

the first term of eq. 2 can be easily computed at run time. In eq. 9, I is the average ionization potential of the material under consideration, and δ_i is the density effect for the level under consideration (all other symbols are of straightforward interpretation). Adopting for $d\sigma_\delta/dT_e$, the proper expressions for spin 0,1/2,1 particles [11] for heavy charged particles, and the Möller and Bhabha cross sections for electrons and positrons, expressions 4 and 5 are straightforward analytic integrations which can be easily run time evaluated with minimal CPU effort.

The algorithm adopted in FLUKA exploits the above model, and makes use of two $(L+1)$ distinct discrete levels for elements (compounds/mixtures), that is the K-shell whose oscillator strength can be assumed [10] to be:

$$f_{jK-shell} = \frac{2\rho_j N_A}{n_e A_j}$$

and all the rest whose energy and strength can be derived from the known energy and strength of the K-shell and the known average ionization potential of the material using eqs. 9 and 10.

Once for a given particle, energy, step length and δ threshold combination, the cumulants of the energy loss distribution are known, the next problem is how to sample from a distribution of given cumulants/moments. This has been accomplished in FLUKA making use of the expansions given in [7] for transforming a gaussian random variate into a variate of given cumulants. The recipe has been implemented up to the 6th order (\rightarrow the first 6 moments of the energy loss distribution are reproduced) and works fine provided the distribution is not dramatically non-gaussian, in order to ensure the proper convergence of the expansion. This last condition can be restored when required, by explicitly producing the “ δ ” rays (typically one or two) between T'_{min} and T_{min} with a suitable T'_{min} , and adding their energy to that computed by the energy loss distribution truncated at T'_{min} .

While the present statistical approach is to our knowledge original and never published before, two technical aspects benefited from works found in the literature. In particular the way of reducing the non-gaussian tails has been inspired by ref. [12], even though our algorithm has no longer any need for relying on a gaussian approximation of the remaining distribution and directly incorporates in a coherent framework distant collisions too, and the suggestion for looking for suitable expansions for distributions no too far from normality stemmed reading ref. [13], where however a different expansion is used.

Two examples of the performances of the FLUKA algorithm are presented in figs. 1. It is worthwhile to stress that similar cumulant approaches based on eq. 1 can be applied to several topics where one is dealing with the sum Poisson distributed independent events. An example is the multiple scattering distribution of charged particles when expressed as a function of the projected angles (to fulfill the additivity requirement). Indeed a development of a new algorithm for multiple scattering based on this approach is foreseen for FLUKA . It will be able to make use in an exact way of any single scattering cross section, as the Goudsmit and Saunderson approach, while keeping the numerical complexity to a manageable level and therefore being applicable to run time calculations with arbitrary step lengths and energies.

2 Neutrino interactions

The final state kinematics in neutrino-nucleus interactions is different and in general more complex than for the free neutrino-nucleon ones. The extent of this difference has never been investigated in detail, although it can heavily affect the results of present and future neutrino experiments. Nuclear effects include initial state effects,

essentially related to nucleon Fermi motion, and final state effects, due to reinteractions of the scattered hadrons in the nucleons, to deflections in the nuclear and Coulomb fields, and to reaction Q-values.

There have been recent proposals [17] for a strong effort for new medium and long baseline experiments to investigate ν oscillations. Within this framework, the ICARUS collaboration found important to develop a description of nuclear effects in ν -nucleus interactions using up-to-date nuclear models. In order to be able to describe neutrino-nucleus interactions within FLUKA, events from free neutrino-nucleon interactions have been generated and used as source for FLUKA. Comparison of the free and the bound final states have been performed.

2.1 Relevant FLUKA aspects

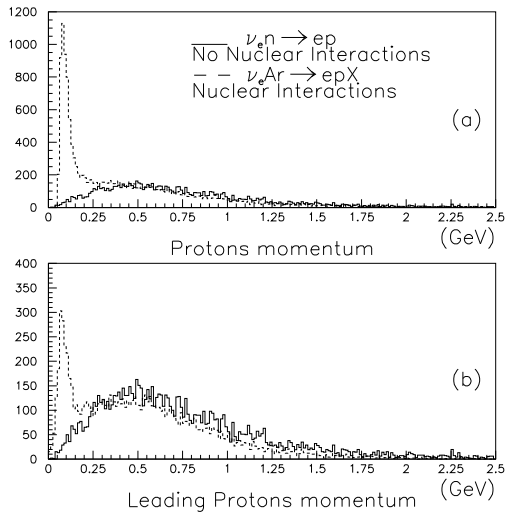


Figure 2: Momentum of final protons in ν interactions (plot (a)); momentum of leading final proton in ν interactions (plot (b))

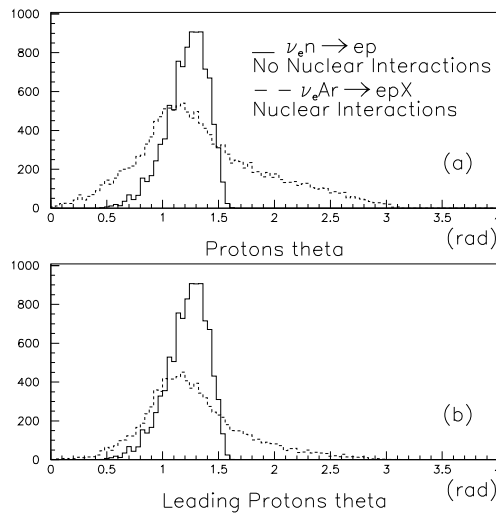


Figure 3: Angular distribution of final protons in ν interactions (plot (a)); angular distribution of leading final proton in ν interactions (plot (b))

Table 1: Final state particles in QE ν ^{40}Ar interactions

final particles	$\langle multiplicity \rangle$	$\langle momentum \rangle$ GeV/c
protons	1.46	0.47
neutrons	1.3	0.16
charged pions	0.025	0.35
pizero's	0.015	0.36
γ -rays	2.36	0.0025

Details about the FLUKA intermediate energy nuclear interaction generator, called PEANUT, can be found elsewhere [16, 15]. We only remind that the reaction mechanism is modelled in PEANUT by explicit intranuclear cascade (INC) smoothly joined to statistical (exciton) preequilibrium emission [19, 18] and followed by evaporation (or fission or Fermi break-up) and gamma deexcitation.

A critical topic in neutrino nucleus interactions is the effect of nuclear Fermi motion. A standard local density approximation Fermi momentum distribution is implemented in PEANUT in order to compute the nucleon mean field:

$$\frac{dN}{dk} = \frac{|k|^2}{2\pi^2} \quad (11)$$

for k up to a local Fermi momentum $k_F(r)$ given by

$$k_F(r) = \left(\frac{3\pi^2}{2} \rho(r) \right)^{\frac{1}{3}} \quad (12)$$

where ρ is the neutron or proton density given by a symmetrized Woods-Saxon [20] shape for $A > 16$ (with the parameters computed according to [21]),

$$\begin{aligned} \rho(r) &= \rho_0 \frac{\sinh(R_0/a)}{\cosh(r/a) + \cosh(R_0/a)} \\ &\approx \frac{\bar{\rho}_0}{1 + \exp \frac{r-R_0}{a}} \end{aligned} \quad (13)$$

and shell model densities [22] are used for light nuclei. On top of the mean field obtained in this way, a gaussian smearing of the momentum distribution of bound nucleons is applied according to uncertainty considerations, with parameters similar to those used in QMD models [23, 24].

Work is in progress to implement high momentum tails in the nucleon momentum distribution according to more or less phenomenological descriptions [25, 26]. According to the literature, these tails are required to explain experimental findings, mainly in electron-nucleus scattering, and they should be related to nucleon-nucleon forces at short distances. They should affect about 10-15% of the nucleons, and they should reflect in the final kinematics as events with a relevant momentum unbalance in the hadron-lepton system. Since, however, the nuclear spectral function for high momenta is centered at high removal energies [25, 26], interactions on high momentum nucleons are expected to be strongly Pauli suppressed and should result in low energy outgoing protons, therefore significantly reducing the net effect of these tails when compared to naive expectations which do not take into account binding and removal energies.

Furthermore, as it will be described later, already the present approach, when included in a coherent nuclear framework, produces significant tails, raising the question about the real amount of genuine high momentum tails required to explain the experimental findings. As soon as the implementation of the high momentum tails will be completed, we hope to be able to investigate these critical problems looking at ordinary hadron and photon induced reactions and comparing with the vast amount of available experimental data for these projectiles.

Another critical issue is the ‘‘coherence’’ length after neutrino interactions, that in PEANUT is assumed to be analogue to the one for elastic or charge exchange hadron-nucleon scatterings. In analogy with the formation zone concept, such interactions cannot be localized better than the position uncertainty connected with the four-momentum transfer of the collision. Reinteractions occurring at distances shorter than the coherence length would undergo interference and cannot be treated anyway as independent interactions on other nucleons. The coherence length is the analogue of the formation time concept for elastic or quasielastic interactions. It has been applied to the secondaries in quasielastic neutrino-nucleon interactions, with the following recipe: given a two body interaction between with four-momentum transfer $q = p_{1i} - p_{1f}$, (where in our case the subscript 1 refers to the *i*initial or *f*final lepton, and 2 to the hadron) the energy transfer seen in a frame where the particle 2 is at rest is given by

$$\Delta E_2 = \nu_2 = \frac{q \cdot p_{2i}}{m_2} \quad (14)$$

From the uncertainty principle this ΔE corresponds to a indetermination in proper time given by $\Delta \tau \cdot \Delta E_2 = \hbar$, that boosted to the lab frames gives a coherence length

$$\Delta x_{lab} = \frac{p_{2lab}}{m_2} \cdot \Delta \tau = \frac{p_{2lab}}{m_2} \frac{\hbar}{\nu_2} \quad (15)$$

2.2 Simulation of Quasi-Elastic ν interactions

As a first step, 10,000 events for ν_τ , ν_μ and ν_e quasielastic interactions on free nucleons have been generated with the wide band neutrino spectrum [27] currently used in the CERN West Area Neutrino Facility for the NO-MAD and CHORUS experiments (the ν_τ spectrum is taken equal to the ν_μ spectrum, while the ν_e spectrum is the expected spectrum for the ν_e contamination in the ν_μ beam).

Final state particles are inserted into Argon nuclei and assumed as initial configurations for PEANUT. The position of the struck nucleon is chosen according to an interaction probability proportional to the local nuclear density. Due to the Fermi motion of the target nucleons, a recorection of the kinematics is necessary. In doing this, the center of mass energy of the free system is preserved, and the incident neutrino direction is fixed; as a consequence all the particle momenta are scaled and rotated.

2.3 Effects on final state kinematics

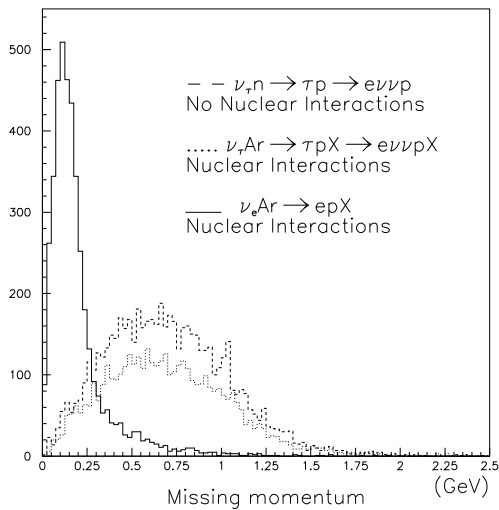


Figure 4: Missing momentum in ν_e bound-nucleon interactions (full line); in ν_τ free-nucleon interactions (dashed line); in ν_τ bound-nucleon interactions (dotted line)

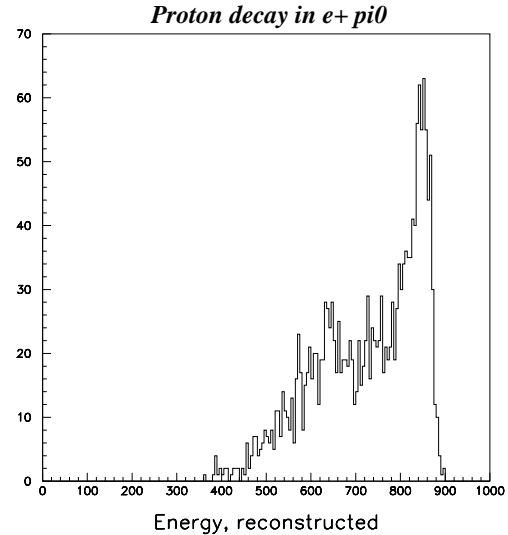


Figure 5: Simulated reconstructed energy (MeV) in ICARUS for $p \rightarrow \pi^0 + e^+$ decays, taking into account nuclear effects

The kinematics of the final states of the free-nucleons and bound-nucleons QE neutrino interactions have been compared. The free-nucleon interactions of the three neutrino species give a lepton and a proton ($\langle p_p \rangle \sim 800$ MeV/c) in the final state, while the bound-nucleons interactions have in the final state a lepton, one (or more) residual nucleus ($\langle p_{res} \rangle \sim 250$ MeV/c and some protons, neutrons, γ -rays and charged and neutral pions with the average multiplicities and momenta given in table 1 (values are very similar for ν_e, ν_μ, ν_τ).

In Fig. 2(a) the momentum spectra of final proton in QE ν_e -free-nucleon interactions and all final protons in QE ν_e -bound-nucleon interactions are compared; in Fig. 2(b) the momentum spectra of the leading final proton in the two interaction types are compared. In Fig. 3(a) the angular spectra of final proton in QE ν_e -free-nucleon interactions and all final protons in QE ν_e -bound-nucleon interactions are compared; in Fig 3(b) the angular spectra of the leading final proton in the two interaction types.

The most important nuclear effect is an apparent missing momentum in the interaction, due to the unseen energy, taken away by the residual nucleus, by neutrons and by undetected low energy particles (γ, p, π). For that reason, while in the free-nucleon ν_e and, ν_μ interactions the missing momentum is zero, in the bound-nucleon interactions the missing momentum is different from zero.

The situation is of course different in the case of ν_τ interactions where a real missing momentum is present ($\langle p_{miss} \rangle \sim 700$ MeV) also in free-nucleon interactions, due to the two neutrinos from the $\tau \rightarrow e$ decay. In this case the missing momentum distribution is not so much modified by nuclear effects.

Calculating the visible momentum in the event summing up the lepton, all protons with $T_p > 60$ MeV, all pions with $T_\pi > 15$ MeV we obtain the plots of Fig. 4, where the distribution of missing momentum for ν_e QE events on bound nucleon is compared to the distributions of missing momentum for ν_τ QE events on free and bound nucleons.

3 Nucleon decays

One of the main goal of the ICARUS experiment is the detection of (possible) nucleon decay events. The peculiar characteristics of the experiment make it able to establish the reality of nucleon decays even on the basis of single events due to its capability of fully reconstructing the 3D pattern of the event itself. It is therefore of mandatory importance to understand in a realistic way the distortions due to the nuclear medium on the nucleon decay products.

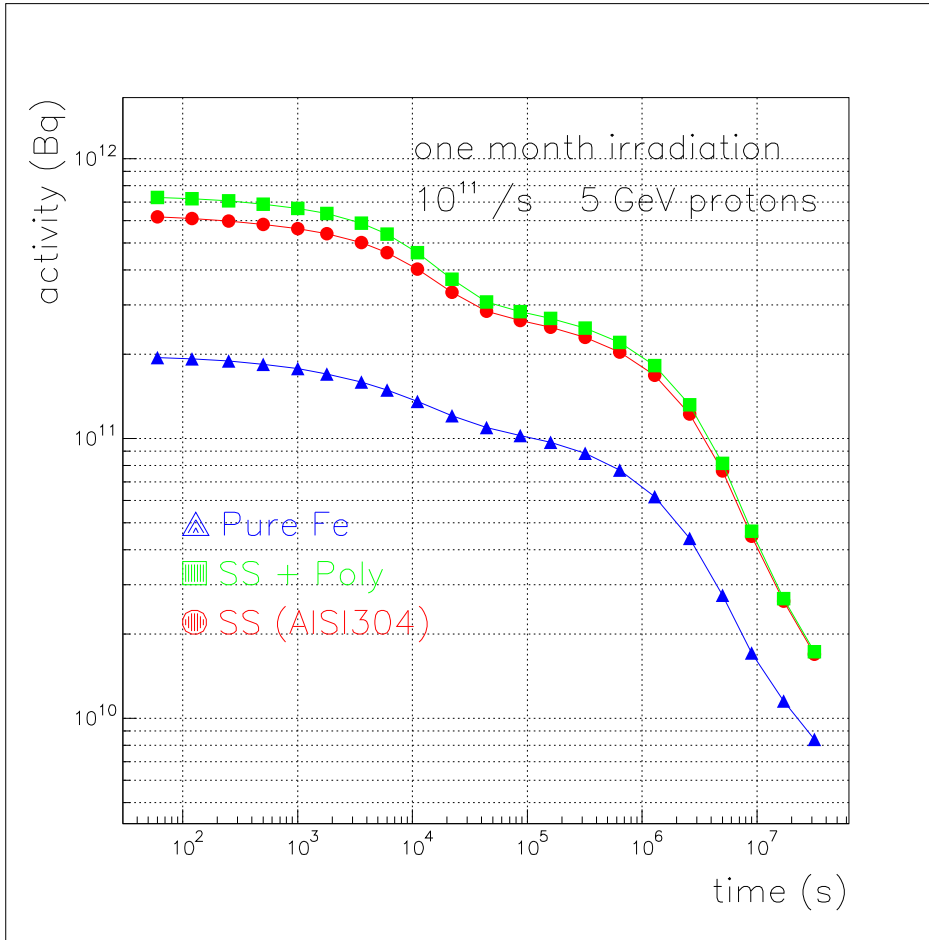


Figure 6: Cooling curves for residual activity for 3 different Stainless Steel and Iron targets (see text)

This task too has been tackled with FLUKA, implementing nucleon decays again into the PEANUT event generator. A realistic nuclear model, which includes multibody processes, like pion absorption, is a key element since most decay events take place deep inside the nucleus core. Indeed significant differences in final state kinematics have been found compared with simpler approaches where for example pion absorption was not properly taken into account. The implementation of nucleon decays is very similar to that of neutrino interactions, with the simplification that the starting event is now a plain phase body decay of a randomly chosen nucleon into the selected decay channel.

As an example in fig. 5 the simulated reconstructed energy for the $p \rightarrow \pi^0 + e^+$ decay is shown. For a free proton this plot would appear like a gaussian centered around the proton mass (938 MeV) due to the three EM showers originating from the positron and the two photons coming from the π^0 . These showers would be reconstructed with a very narrow spread due to the good EM energy resolution of ICARUS which acts as a fully sensitive liquid Argon calorimeter.

4 Residual nuclei production and scoring

The FLUKA ability in predicting residual nuclei has been substantially strengthened thanks to three major improvements:

- The evaporation part of the nuclear interaction models has been rewritten from scratch adopting a sampling scheme for the emitted particle spectra which no longer makes any maxwellian like approximation and which includes sub-barrier effects. Gamma competition has been introduced too.

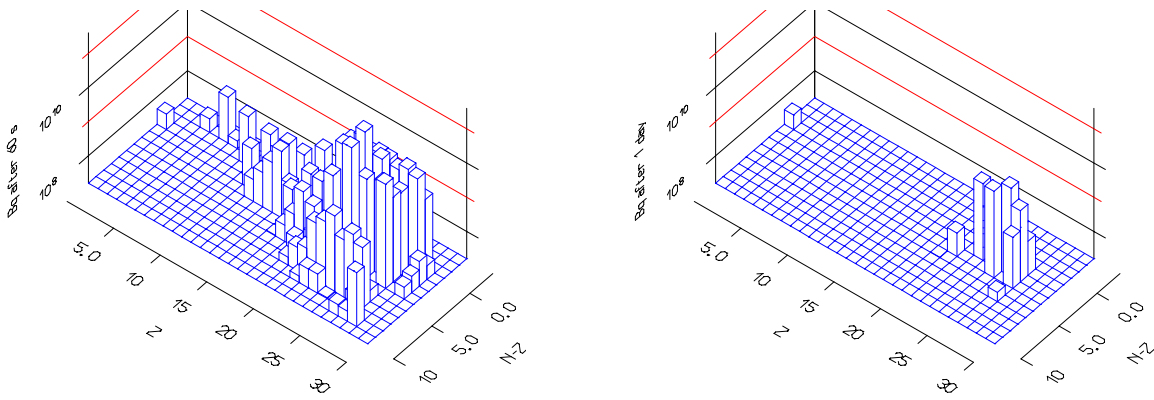


Figure 7: Computed residual activities (Bq) as a function of the isotope atomic number Z and neutron excess $N-Z$ for an AISI304 target irradiated by 10^{11} 5 GeV protons s^{-1} for one month: after 60 s (left) and after 1 year (right)

- Residual nuclei yields due to neutron interactions at energies below 20 MeV are now available, due to a new version of the group library which includes residual nuclei informations whenever they can be derived from the basic nuclear data
- Fission fragment yields due to neutron interactions below 20 MeV are also available, due to the coupling on-line with a general sampling algorithm [28] for binary and ternary fission fragments based on the most recent nuclear data files

A simple postprocessor is available which can evolve the residual nuclei distribution obtained from FLUKA , according to given irradiation and cooling times.

As an example of residual nuclei calculations including yields due to low energy neutrons, the cooling curve of a 1 m long, 40 cm radius AISI304 cylinder irradiated by 10^{11} 5 GeV protons s^{-1} for one month, is shown in fig. 6 together with the corresponding ones for a pure iron target and for a target lined on the external surface with polyethylene respectively. The activities of the isotopes surviving after 60 s and 1 year after the end of the irradiation are shown in fig. 7. The peaks due to ^{54}Mn , ^{55}Fe and ^{27}Co can be easily identified after one year of cooling.

5 Conclusions

The field of applications of FLUKA is becoming wider and wider, with a growing emphasis towards description and design of physics experiments. The capabilities of the code in the detailed description of both EM and hadronic processes from few tens of MeV up to atmospheric showers proved to be a key issue in many applications, and were even more enlightened when compared with standard codes for detector simulations. (see also [29]).

The code resulted to be useful also for the field of rare event detection (nucleon decay, neutrino induced events, etc.), where the very demanding constraints on physics description cannot be matched at present by standard codes like GEANT [30].

Acknowledgements

The authors acknowledge the important contributions of D. Cavalli and A. Rubbia to the developments concerning ICARUS, and that of F. Carminati who kindly provided the fission fragment code and gave a substantial support on many items.

References

- [1] A. Ferrari, T. Rancati, and P.R. Sala, this conference
- [2] L. Landau, J. Phys. USSR **8**, 201, (1944)

- [3] P.V. Vavilov, Sov. Phys. JETP **5**, 749 (1957)
- [4] H. Bichsel, Rev. Mod. Phys. **60**, 663 (1968)
- [5] O. Blunck, and K. Westphal, Z. Phys. **130**, 641 (1951); P. Shulek et al., Sov. J. Nucl. Phys. **4**, 400 (1967)
- [6] S.M. Seltzer, Appl. Radiat. Isot. **42**, 917 (1991)
- [7] A. Stuart, J.K. Ord, “Kendall’s Advanced Theory of Statistics”, Vol. I (Distribution Theory), Charles Griffin & Co. Ltd, London (1987)
- [8] A. Ferrari, and P.R. Sala, to be submitted to Nucl. Instr. Meth.
- [9] V.A. Chechin, and V.C. Ermilova, Nucl. Instr. Meth. **136**, 551 (1976)
- [10] R.M. Sternheimer, ADNDT **30**, 261 (1984) and references therein
- [11] E.A. Uehling, Ann. Rev. Nucl. Sci. **4**, 315 (1954)
- [12] K. Lassila-Perini, and L. Urban, Nucl. Instr.Meth., **A362**, 416 (1995)
- [13] A. Rotondi, and P. Montagna, Nucl. Instr. Meth. **B47**, 215 (1990)
- [14] J.F. Bak et al., Nucl. Phys. **B288**, 681 (1987)
- [15] A. Fassò, A. Ferrari, J. Ranft, and P.R. Sala, “Proc. of the “Specialists’ Meeting on Shielding Aspects of Accelerators, Targets & Irradiation Facilities”, Arlington, April 28-29 1994, published by OECD/NEA, 287 (1995)
- [16] A. Ferrari, and P.R. Sala, “The Physics of High Energy Reactions”, in Proceedings of the “Workshop on Nuclear Reaction Data and Nuclear Reactors Physics, Design and Safety”, International Centre for Theoretical Physics, Miramare-Trieste, Italy, 15 April–17 May 1996, World Scientific in press
- [17] J.P. Revol, A. Rubbia, C. Rubbia, P. Picchi, F. Pietropaolo, C. Montanari, F. Sergiampietri, D. Cavalli, A. Ferrari, P.R. Sala, S. Ragazzi, ICARUS-TM-97/01
- [18] J. J. Griffin, Phys. Rev. Lett. **17**, 438 (1966)
- [19] E. Gadioli and P. E. Hodgson, “Pre-equilibrium Nuclear Reactions”, (Clarendon Press, Oxford, 1992)
- [20] M.E. Grypeos, G.A. Lalazissis, S.E. Massen and C.P. Panos, J. Phys. **G 17** (1991) 1093.
- [21] W.D. Myers, “Droplet Model of Atomic Nuclei”, IFI/Plenum, New York, 1977
- [22] L.R.B. Elton, Nuclear sizes, Oxford University Press, 1961
- [23] K. Niita et al., Phys. Rev. **C52**, 2620 (1995)
- [24] C.Hartnack, and J. Aichelin, Phys. Rev. **C49**, 2801 (1995)
- [25] C. Ciofi degli Atti, and S. Simula, Phys. Rev. **C53**, 1589 (1996)
- [26] P. Fernández de Córdoba et al., Nucl. Phys. **A611**, 514 (1996)
- [27] A. Rubbia, private communication
- [28] Federico Carminati, private communication
- [29] A. Ferrari, and P.R. Sala, Internal note ATLAS-PHYS-no-086, June 1996
- [30] R. Brun et al., GEANT3, CERN DD/EE/84-1 (1987).